Supporting Electronic Information

Tuning the Electrocatalytic Nitric oxide Reduction activity of Copper through Alloying with Nickel for NH_3 production at low Overpotentials

*Harish Reddy Inta, Dinesh Dhanabal, Song Yuyeon and Sangaraju Shanmugam**

Department of Energy Science and Engineering, Daegu Gyeongbuk Institute of Science & Technology (DGIST), Daegu 42988, Republic of Korea

*E-mail: sangarajus@dgist.ac.kr

Experimental Section

Electrochemical Measurements

For the electrode preparation, the homogenous catalyst ink was prepared by dispersing the catalyst powder (2 mg) in isopropanol (240 µL), DIW (40 µL), and 5 wt% Nafion solution (10 µL) with the aid of ultrasonication for 30 min. The catalytic ink was loaded onto the microporous carbon layer of GDL through the brush-coating method and subsequently dried in the oven. The electrocatalytic nitric oxide reduction reaction (NORR) activity of the materials is evaluated through the half-cell studies by using a two-compartment H-type cell. The compartments are separated by an anion exchange membrane which was pretreated with NaCl (to remove the membrane additives) and KOH solutions (to convert the membrane into OH^- form), respectively. The electrochemical measurements were performed by filling nearly 80% of the cell volume with 1M KOH electrolyte (85 ml) in both compartments. The catalyst coated GDE, Hg/HgO (1M KOH), and Graphite rod were used as working, reference, and counter electrodes. Prior to the measurements the Ar gas was purged into the electrolyte for 30 min to remove the dissolved oxygen. Throughout the NORR studies, the Ar flow was continued through the headspace (over the electrolyte level) of the cell to prevent the NO_2 formation (resulting from the reaction between nitric oxide and the residual oxygen). For NORR studies, the electrolyte was saturated with 99.9% NO (flow rate:1 sccm) for 30 minutes. The linear sweep voltammetry was performed in the voltage window of +0.7 V to -0.7 V (vs. RHE) at a scan rate of 5 mVs^{-1}. Chronoamperometric (CA) studies were performed at various potentials with regular intervals. All the potential values are converted into RHE scale by using the following Nernst equation.

$$E_{RHE} = E_{working} + E_{Hg/HgO} + 0.059\ pH\ ;\ E_{Hg/HgO} = +0.11\ V$$

After the CA studies for 1 hour, 2 ml of electrolyte (dissolved with NORR products) was collected and used to identify and quantify the electrochemically synthesized NORR products such as NH_3, and N_2H_4 by using UV-visible spectroscopy and ^1H NMR methods. The Zn-NO battery was assembled by using the GDE coated $Cu_{75}Ni_{25}$@NC as cathode and polished Zn plate as anode. The anodic and cathodic compartments are filled with 1M KOH, and an anion exchange membrane (AEM) was used as a separator. Prior to the Zn-NO battery performance evaluation the catholyte was saturated with 99.9% NO, and the flow was maintained through battery operation.

Product Quantification

Colorimetric Quantification of NH_3 (Indophenol Blue Method)

The indophenol blue method was used to estimate the NH_3 yields. 2 mL of aliquot collected after 1 h of electrolysis was mixed with 2 mL of Reagent A (1 M NaOH containing 5 wt % salicylic acid and 5 wt % trisodium citrate dihydrate), 1 mL of Reagent B (0.05 M sodium hypochlorite), and 200 μL of Reagent C (1 wt % sodium nitroprusside) and the result mixture is incubated in dark for 1h. After that, the samples are subjected to the UV-visible spectroscopy to record the absorption spectrum in the wavelength range of 500-800 nm, and the peak absorbance at 655 nm is considered to calculate the ammonia yield. Similarly, the NH_3 calibration plot was obtained by recording the absorbance values of known ammonium chloride solutions prepared in 1M KOH (Fig. S13).

^1H NMR Quantification of NH_3

For quantifying the ammonia through ^1H NMR, 400 μL of aliquot was mixed with 100 μL of 4 M H_2SO_4 and 50 μL of DMSO-d6. The internal standard 100 μL of Maleic acid (2500 μM) is added into the above solution mixture. The ^1H NMR spectrum acquisition with ordinarily pulse sequence (zg30) could not produce any characteristic triplet peaks of ammonia, which could be

due to the dominant proton signals raised from the aqueous solvent. By employing the pulse sequence (zgesgp) with 256 scan acquisition, the solvent peak got suppressed and the clear triplet peaks of ammonia were obtained. The Ammonia was quantified by integrating the triplet peaks with respect to the standard maleic acid peak (6.25 δ). The standard NH_3 calibration plot was obtained by recording ^1H NMR spectrum of known ammonium chloride solutions prepared in 1M KOH (Fig. S14).

Colorimetric Quantification of N_2H_4 (Watt and Chrisp Method)

The Watt and Chrisp method is used to identify and quantify the hydrazine side product. Initially, the color reagent was prepared by dissolving 5.99 g of para-(dimethylamino) benzaldehyde in 30 mL of concentrated HCl and 300 mL of ethanol. 2 mL of the aliquot is mixed with 3 mL of DIW and 5 mL color reagent and incubated for 10 min in dark. The UV-visible spectrum of the above solution mixture is recorded in the wavelength range of 420-520 nm and the peak absorbance at a wavelength of 455 nm was considered to calculate the formed hydrazine. Similarly, the N_2H_4 calibration plot was obtained by recording the absorbance values of known N_2H_4 solutions prepared in 1M KOH (Fig. S15).

Equations used for the estimation of NH_3 yield rates and FE_{NH3}

1. *Average Ammonia yield rate (Y_p)*

The average yield rate (Y_p) of ammonia produced from electrocatalytic NORR process was calculated by the following equation:

$$\textit{Average yield rate } (Y_p) = \frac{(C_{product} \times V)}{A \times t \times M_w}$$

Where Y_p is the mean rate of NH_3 formation (μmol cm^{-2} h^{-1}), $C_{product}$ is the concentration of NH_3 formed (estimated by the Indophenol-blue method) after the electrolysis (μg mL^{-1}), V is the total volume of electrolyte in the cathodic compartment (mL), A is the area of cathode (cm^2), t is the electrolysis time (h), and M_w is the molar mass of NH_3 (g mol^{-1}).

2. *Faradaic Efficiency (FE) of NH_3*

The Faradaic Efficiency (FE) of ammonia was calculated by the following equation:

$$FE\,(\%) = \frac{(n \times F \times C_{product} \times V \times 10^{-4})}{M_w \times Q}$$

Where n is the number of electrons transferred during NORR to NH_3 (5 electrons), F is the Faraday constant (96485 C mol^{-1}), $C_{product}$ concentration of NH_3 formed after the electrolysis (μg mL^{-1}), V is the total volume of electrolyte in the cathodic compartment (mL), M_w is the molar mass of NH_3 (g mol^{-1}), and Q is the quantity of charge consumed during the electrolysis (C).

Table S1 Rietveld refinement parameters of the all the electrocatalysts.

Cu_{100}@NC **$\chi2 = 2.24$**	**Name**	**Type**	**x**	**y**	**z**	**frac**
0	Cu1	Cu^0	0.00000	0.00000	0.00000	0.2000
1	Cu2	Cu^0	0.00000	0.00000	0.00000	0.8000
$Cu_{75}Ni_{25}$@NC **$\chi2 = 2.10$**	**Name**	**Type**	**x**	**y**	**z**	**frac**
0	Ni1	Ni^0	0.00000	0.00000	0.00000	0.2500
1	Cu1	Cu^0	0.00000	0.00000	0.00000	0.7500
$Cu_{50}Ni_{50}$@NC **$\chi2 = 1.76$**	**Name**	**Type**	**x**	**y**	**z**	**frac**
0	Ni1	Ni^0	0.00000	0.00000	0.00000	0.5000
1	Cu1	Cu^0	0.00000	0.00000	0.00000	0.5000
$Cu_{25}Ni_{75}$@NC **$\chi2 = 2.22$**	**Name**	**Type**	**x**	**y**	**z**	**frac**
0	Ni1	Ni^0	0.00000	0.00000	0.00000	0.7500
1	Cu1	Cu^0	0.00000	0.00000	0.00000	0.2500
Ni_{100}@NC **$\chi2 = 2.10$**	**Name**	**Type**	**x**	**y**	**z**	**frac**
0	Ni1	Ni^0	0.00000	0.00000	0.00000	0.5000
1	Ni2	Ni^0	0.00000	0.00000	0.00000	0.5000

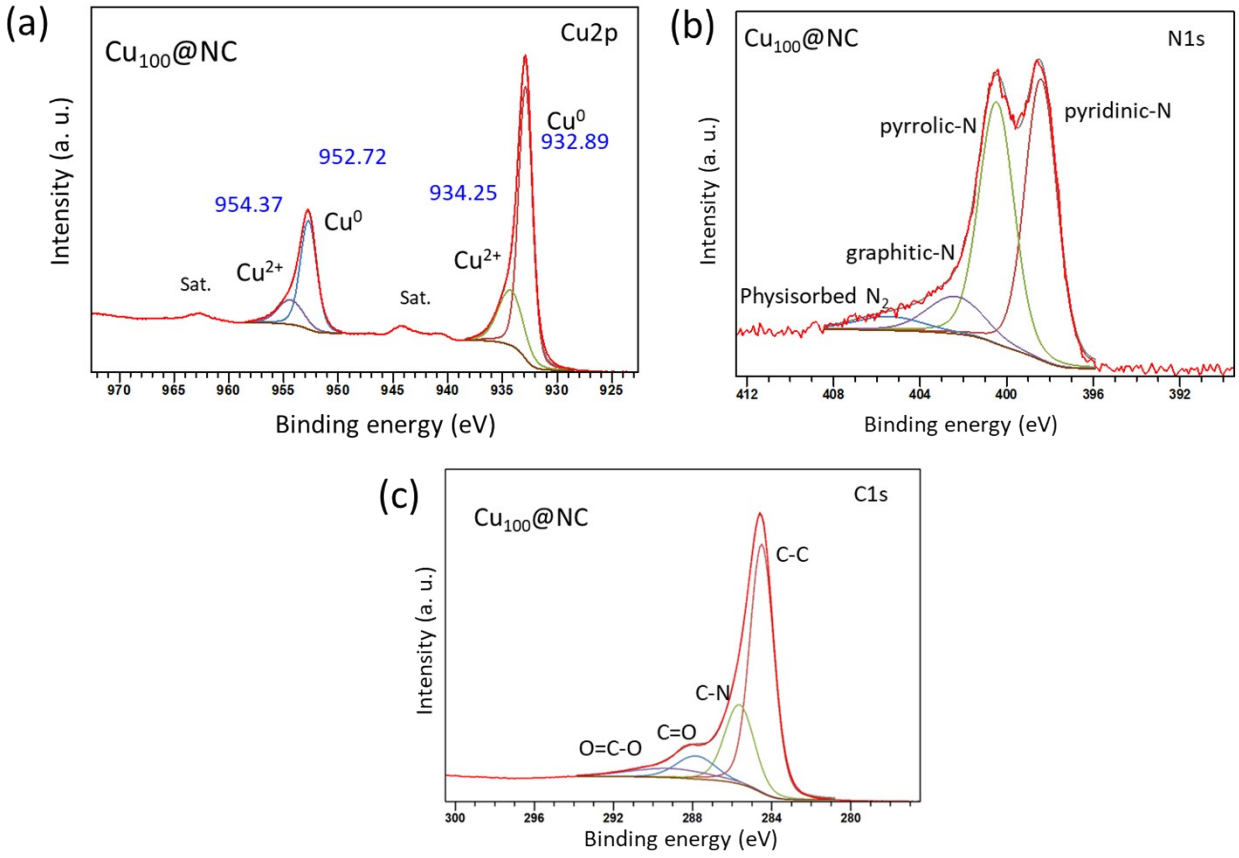

Fig. S1 Deconvoluted XPS spectra of (a) Cu2p, (b) N1s, and (c) C1s of Cu_{100}@NC.

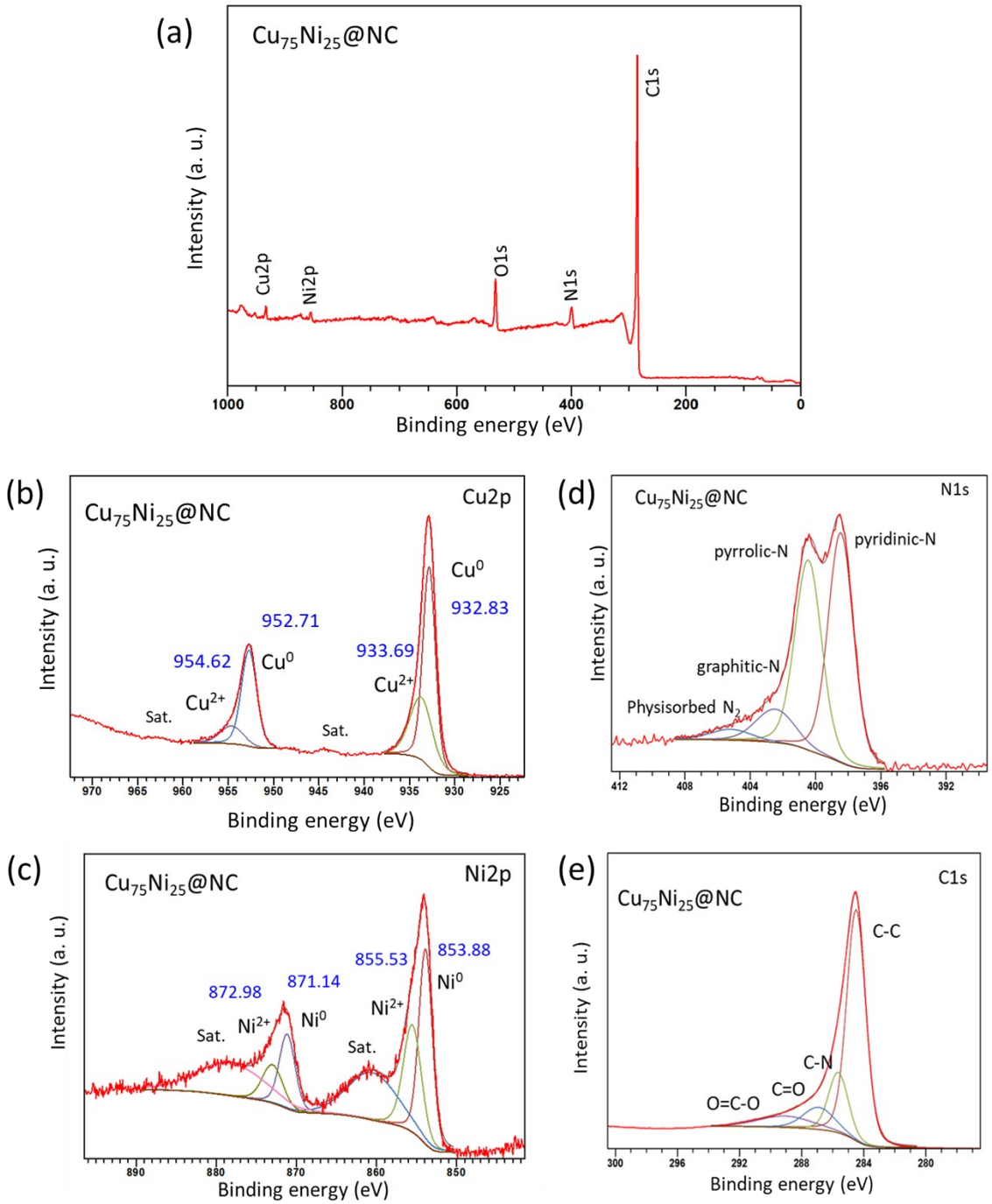

Fig. S2 (a) XPS survey scan of $Cu_{75}Ni_{25}$@NC. The deconvoluted XPS spectra of (b) Cu2p, (c) Ni2p, (d) N1s, and (e) C1s of $Cu_{75}Ni_{25}$@NC.

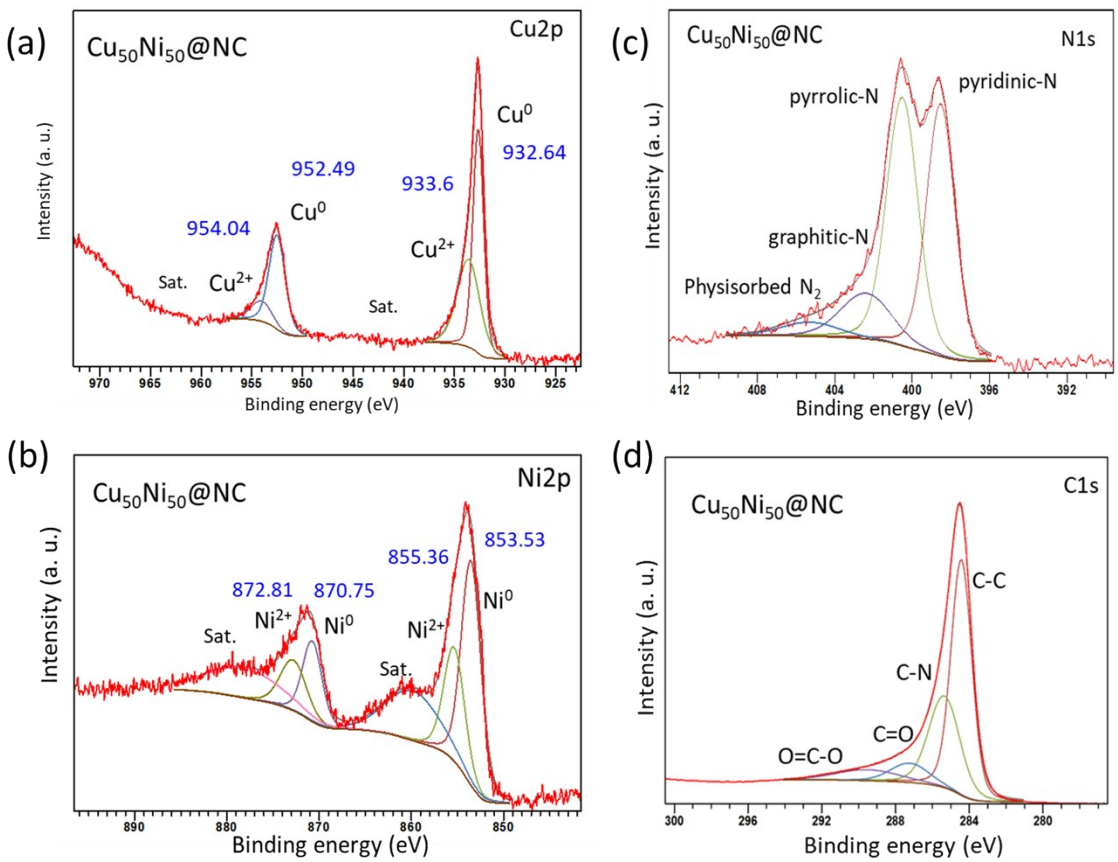

Fig. S3 Deconvoluted XPS spectra of (a) Cu2p, (b) Ni2p, (c) N1s, and (d) C1s of $Cu_{50}Ni_{50}$@NC.

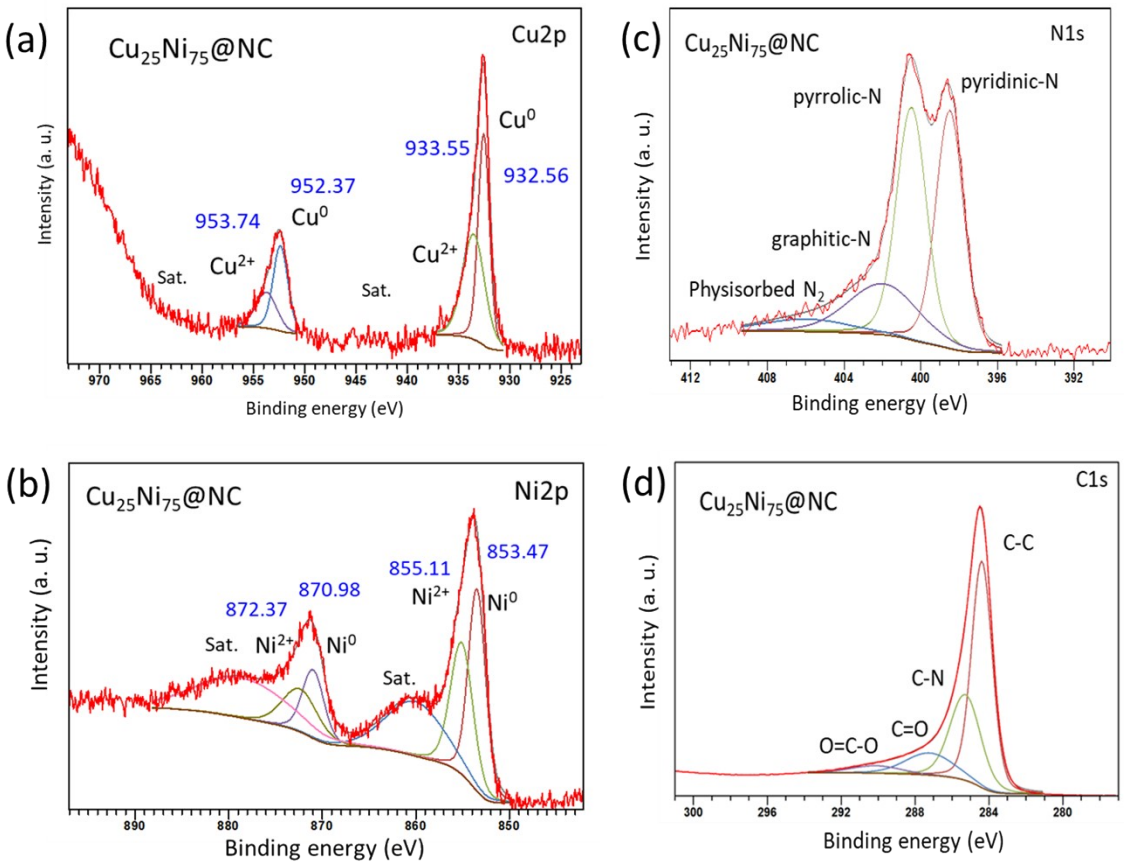

Fig. S4 Deconvoluted XPS spectra of (a) Cu2p, (b) Ni2p, (c) N1s, and (d) C1s of $Cu_{25}Ni_{75}$@NC.

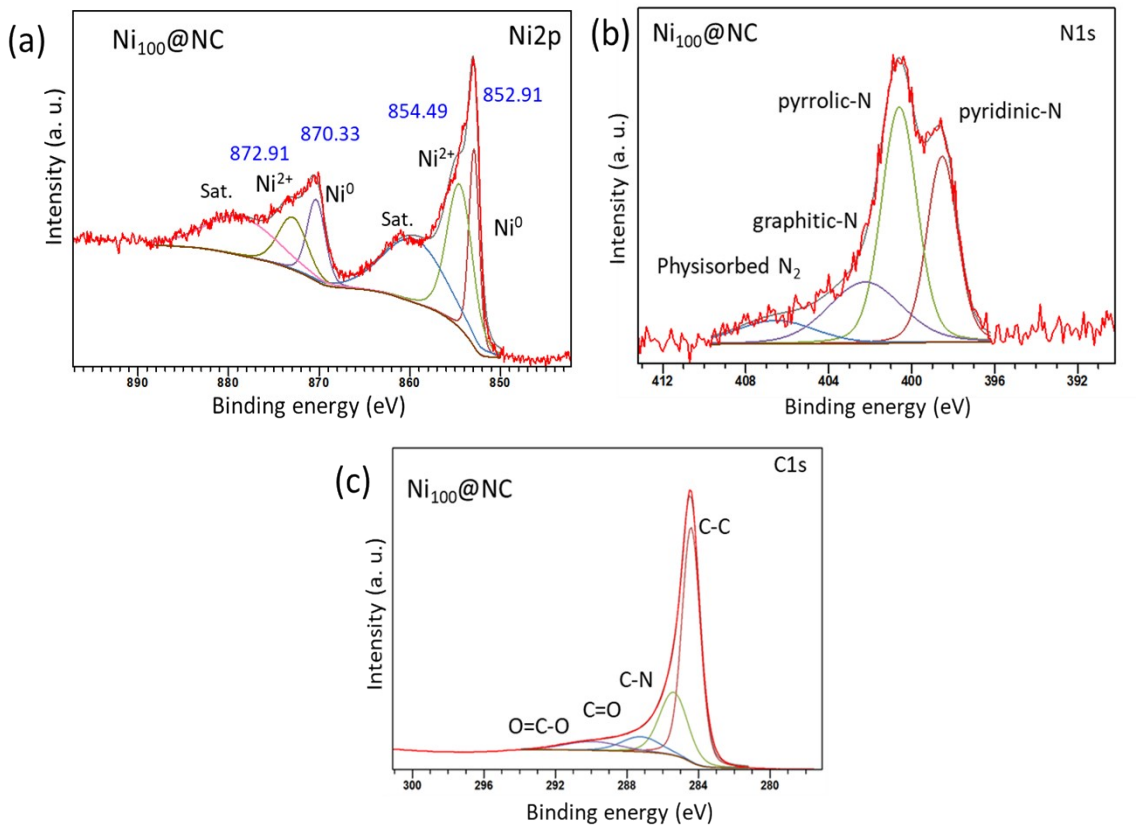

Fig. S5 Deconvoluted XPS spectra of (a) Ni2p, (b) N1s, and (c) C1s of Ni_{100}@NC.

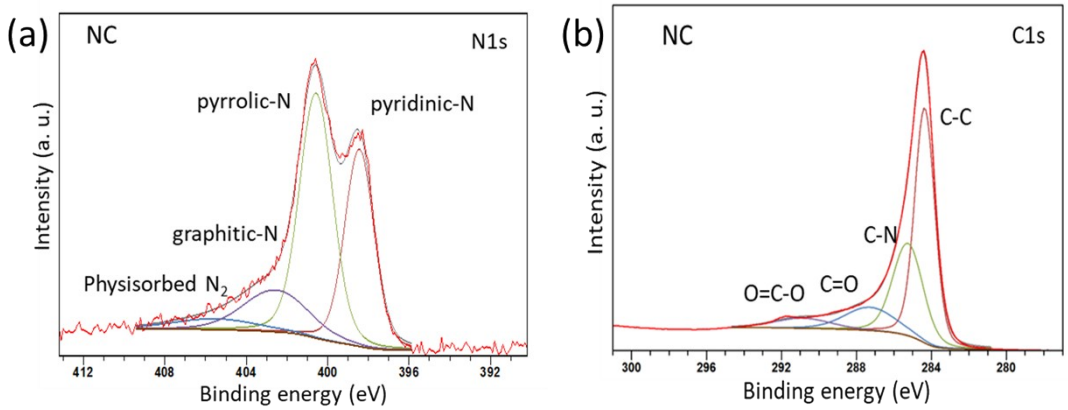

Fig. S6 Deconvoluted XPS spectra of (a) N1s, and (b) C1s of NC.

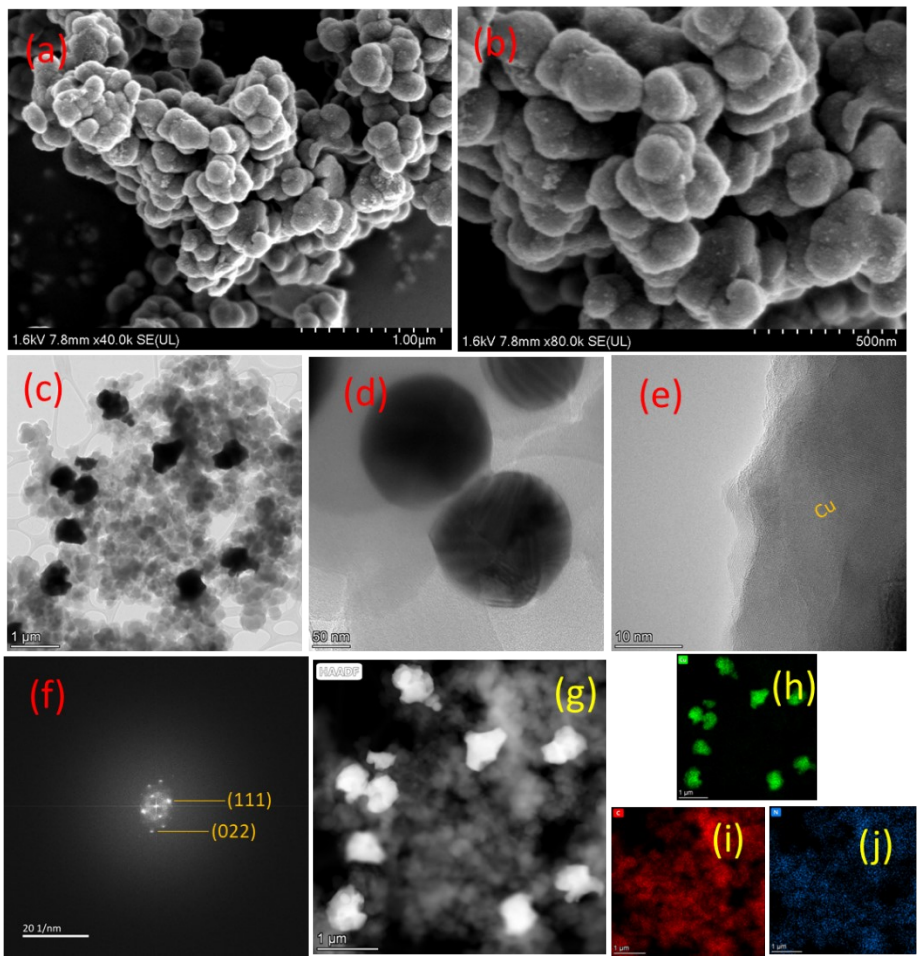

Fig. S7 (a-b) FESEM, (c-d) TEM images of Cu_{100}@NC. (e) HRTEM image and (f) the corresponding FFT pattern of Cu_{100}@NC. (g) HAADF image and (h-j) elemental mapping of Cu_{100}@NC.

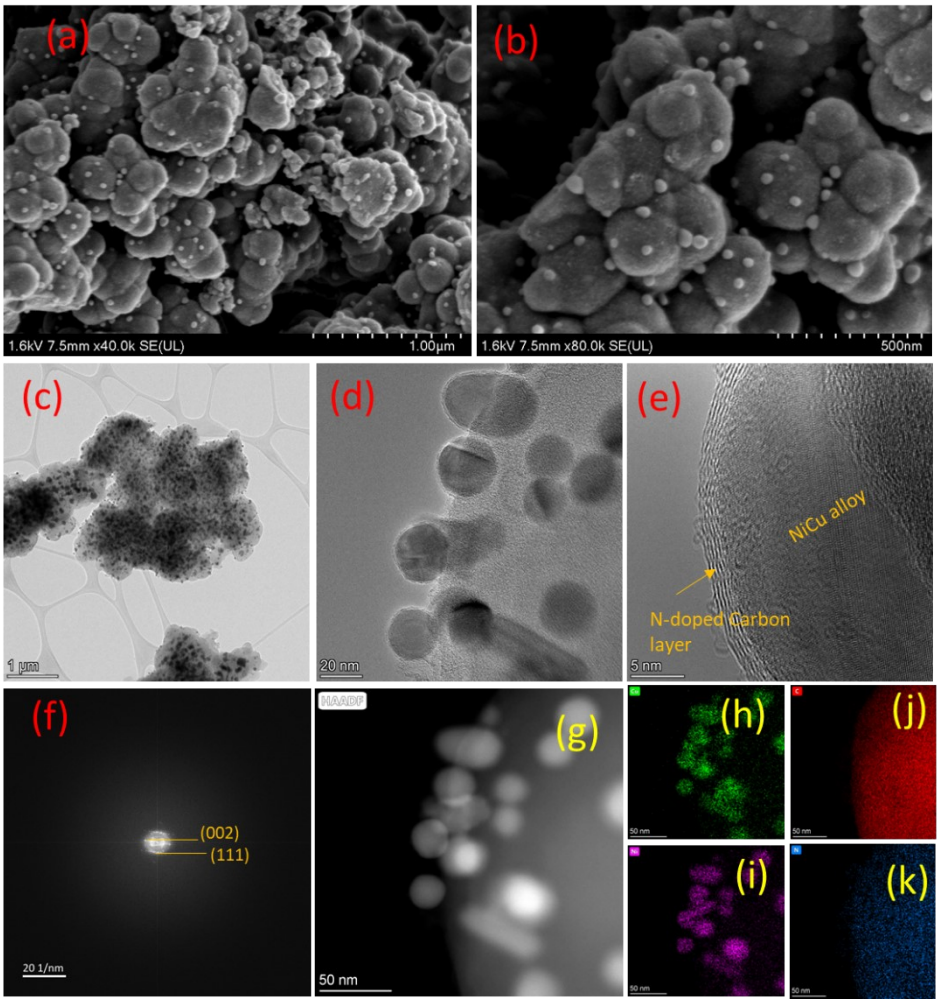

Fig. S8 (a-b) FESEM, (c-d) TEM images of $Cu_{50}Ni_{50}$@NC. (e) HRTEM image and (f) the corresponding FFT pattern of $Cu_{50}Ni_{50}$@NC. (g) HAADF image and (h-k) elemental mapping of $Cu_{50}Ni_{50}$@NC.

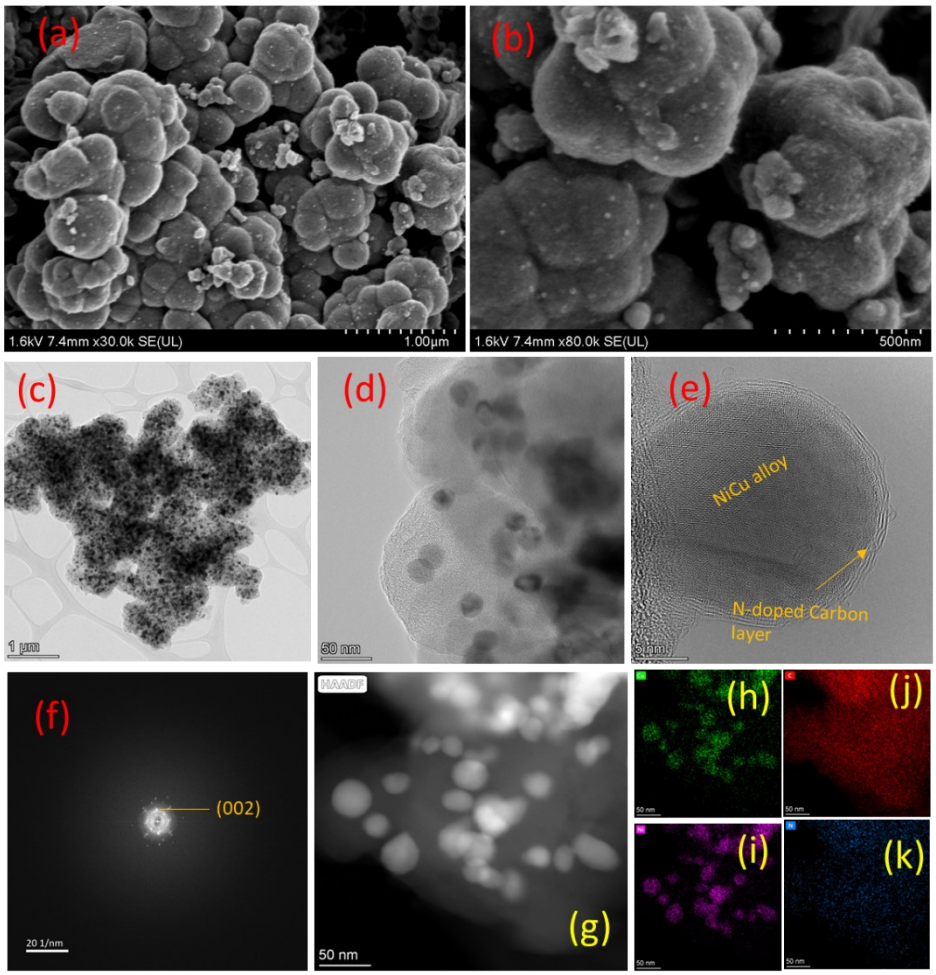

Fig. S9 (a-b) FESEM, (c-d) TEM images of $Cu_{25}Ni_{75}$@NC. (e) HRTEM image and (f) the corresponding FFT pattern of $Cu_{25}Ni_{75}$@NC. (g) HAADF image and (h-k) elemental mapping of $Cu_{25}Ni_{75}$@NC.

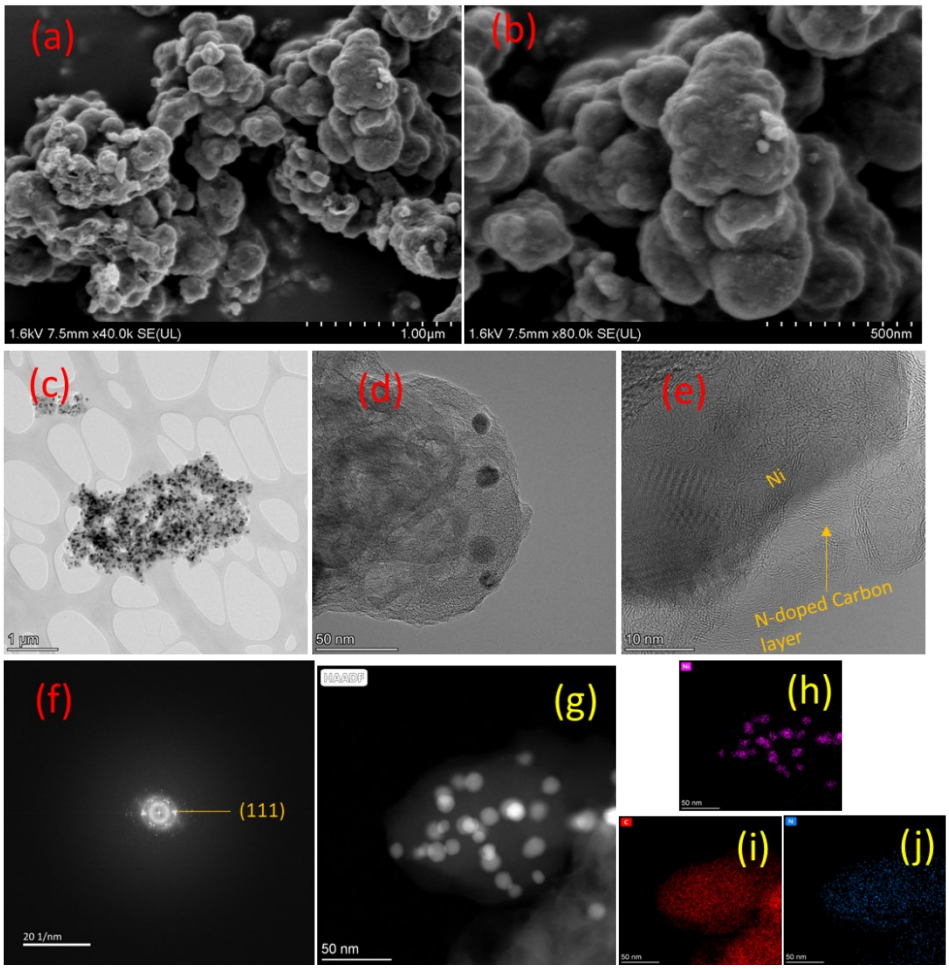

Fig. S10 (a-b) FESEM, (c-d) TEM images of Ni_{100}@NC. (e) HRTEM image and (f) the corresponding FFT pattern of Ni_{100}@NC. (g) HAADF image and (h-j) elemental mapping of Ni_{100}@NC.

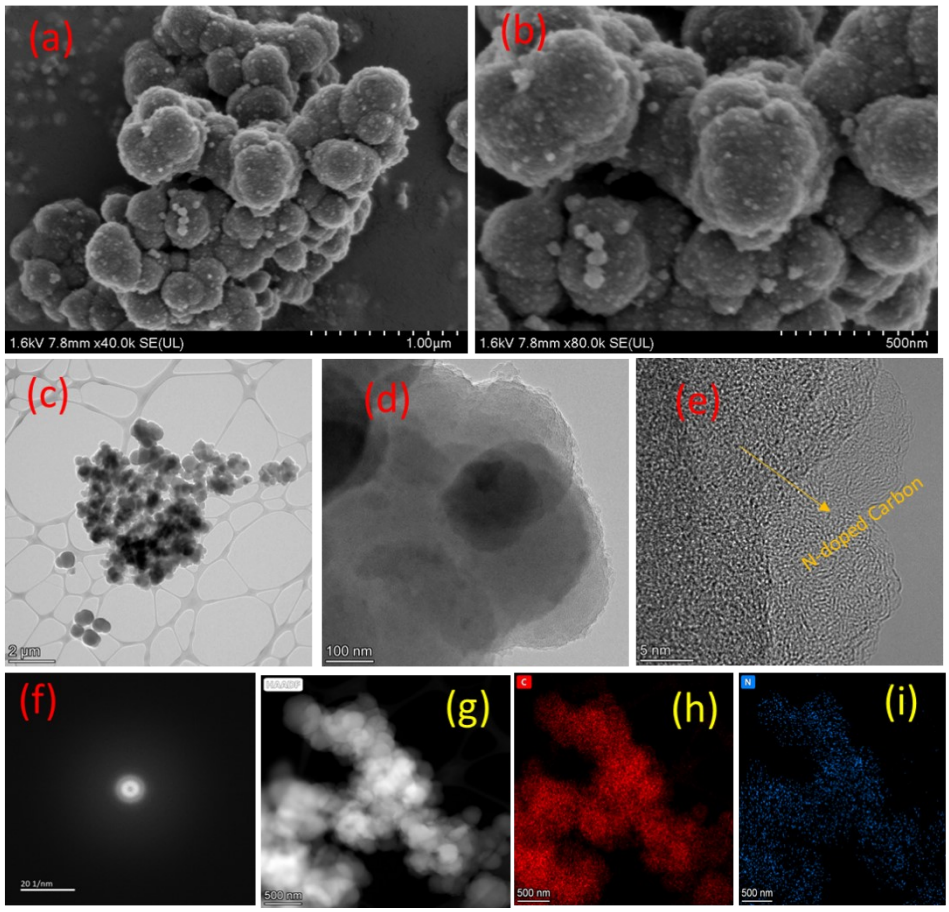

Fig. S11 (a-b) FESEM, (c-d) TEM images of NC. (e) HRTEM image and (f) the corresponding FFT pattern of NC. (g) HAADF image and (h-i) elemental mapping of NC.

Table S2 ICP-OES data of the nanoalloy catalysts.

Sample	Cu (ppm)	Ni (ppm)	Cu (mM)	Ni (mM)	Cu: Ni ratio
$Cu_{75}Ni_{25}$@NC	0.139	0.027	0.0021	0.00046	4.5: 1
$Cu_{50}Ni_{50}$@NC	0.18	0.195	0.0028	0.0033	0.85: 1
$Cu_{25}Ni_{75}$@NC	0.179	0.475	0.0028	0.0080	1: 2.9

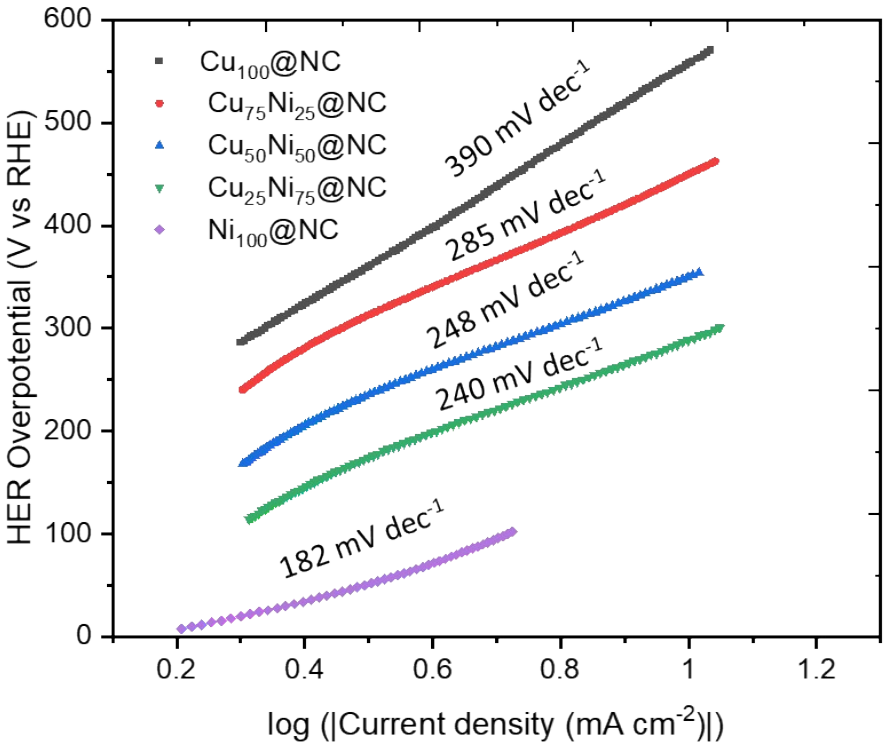

Fig. S12 Tafels plot for all the electrocatalysts.

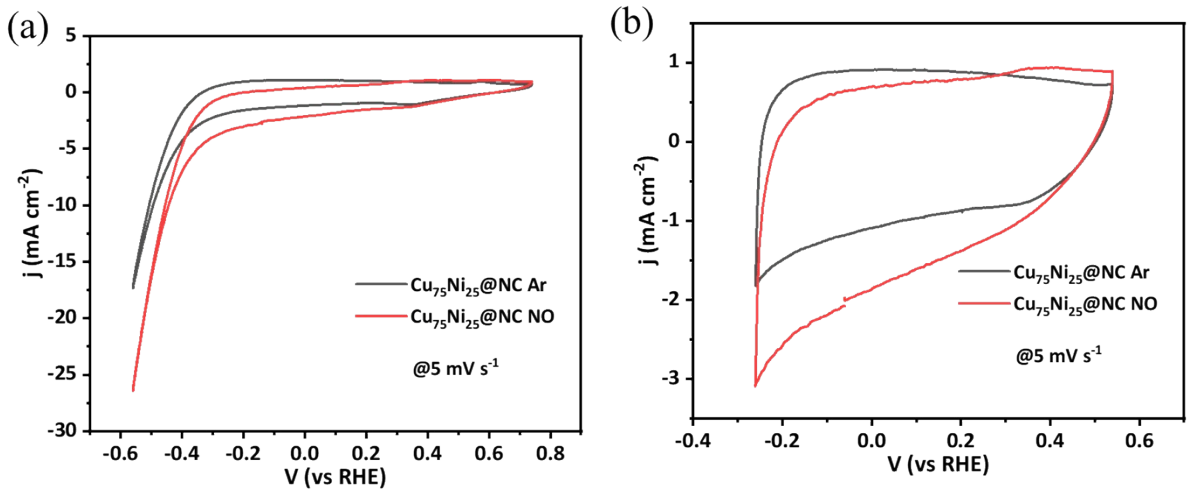

Fig. S13 (a-b) The cyclic voltammograms (CV) of the $Cu_{75}Ni_{25}$@NC near HER region in Ar and NO-saturated electrolyte.

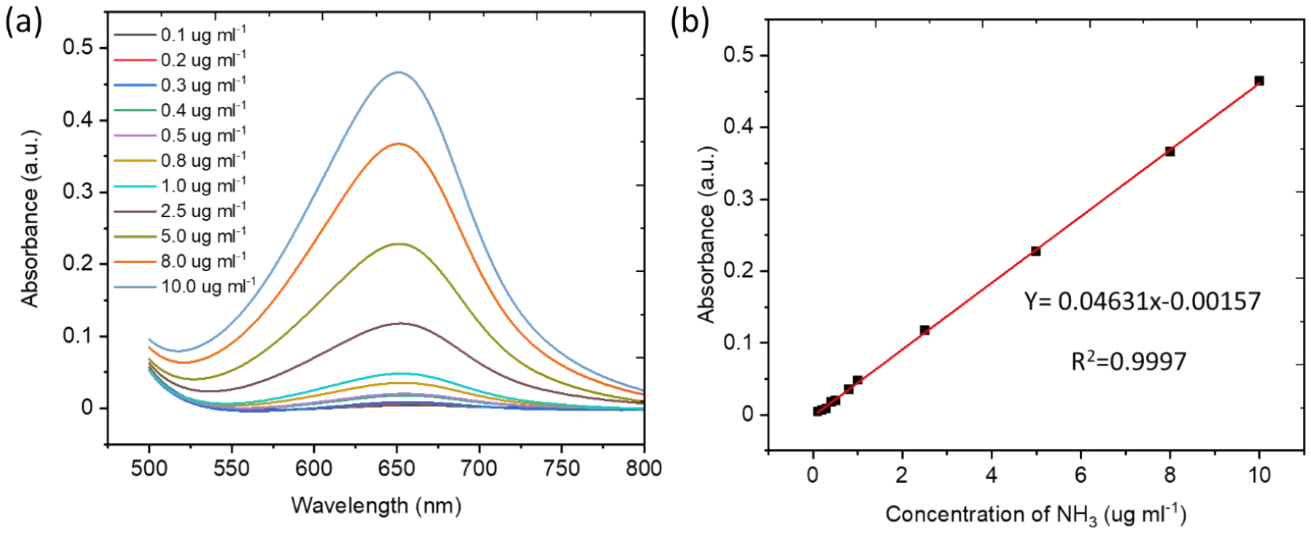

Fig. S14 NH_3 standard calibration plots using Indophenol blue method. (a) UV-visible spectra and (b) Calibration curve of standard NH_3 concentrations.

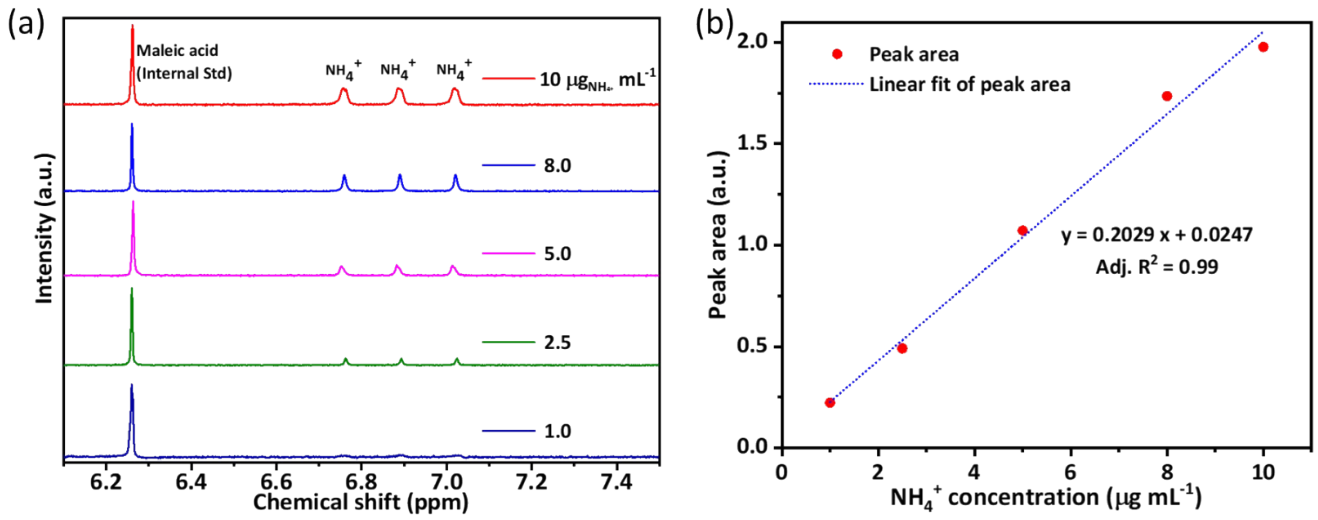

Fig. S15 ^{1}H NMR standard calibration plots for NH_3 (a) ^{1}H NMR spectra and (b) Calibration curve of standard NH_3 concentrations.

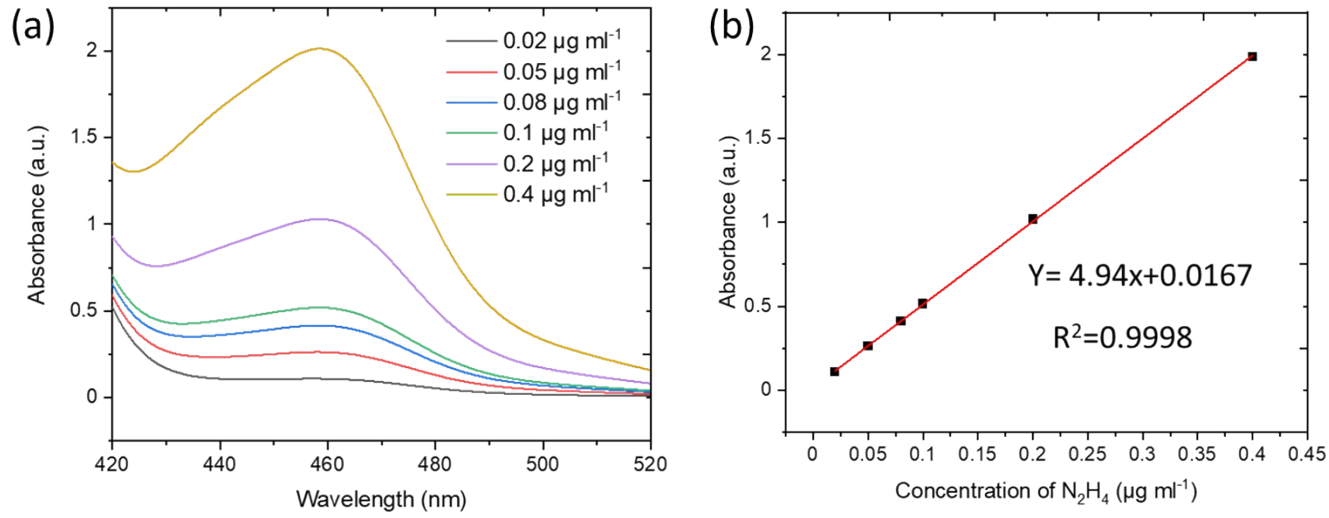

Fig. S16 N_2H_4 standard calibration plots using Watt and Chrisp Method. (a) UV-visible spectra and (b) Calibration curve of standard N_2H_4 concentrations.

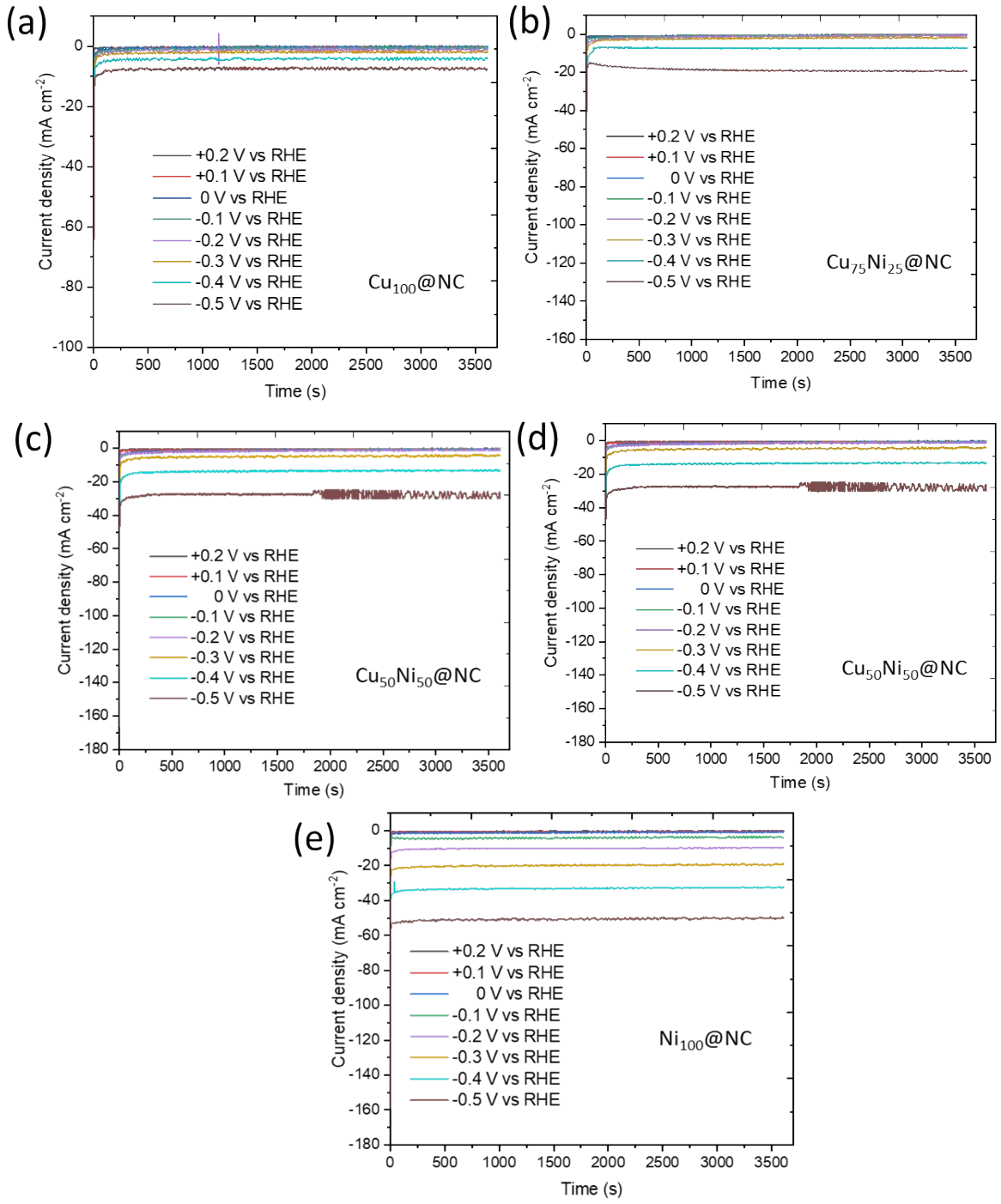

Fig. S17 CA studies (NO medium) of (a) Cu_{100}@NC, (b)$Cu_{75}Ni_{25}$@NC, (c) $Cu_{50}Ni_{50}$@NC, (d) $Cu_{25}Ni_{75}$@NC, and (e) Ni_{100}@NC at various potentials.

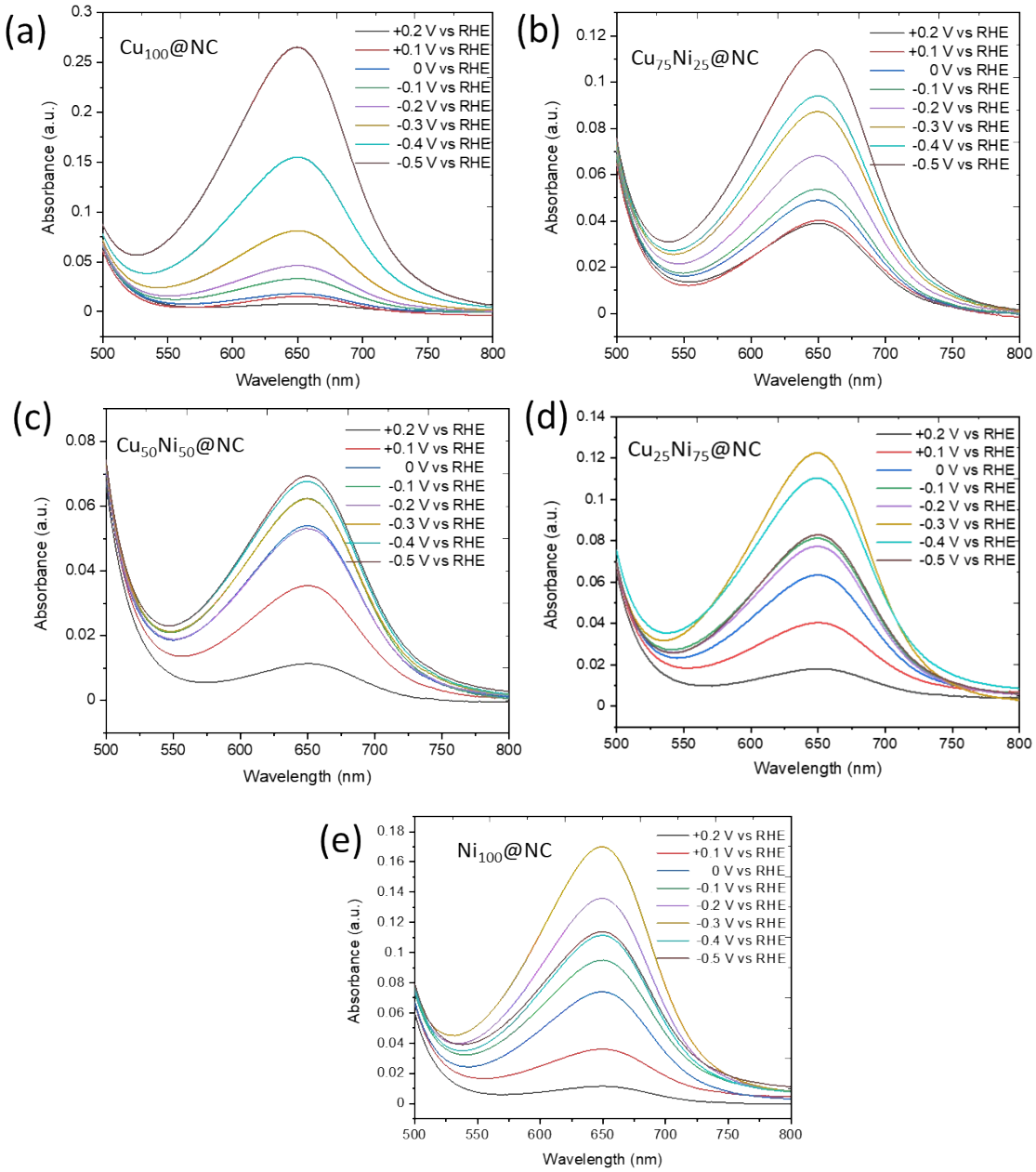

Fig. S18 UV-visible spectra of aliquots collected after 1 h electrolysis of (a) Cu_{100}@NC, (b)$Cu_{75}Ni_{25}$@NC, (c) $Cu_{50}Ni_{50}$@NC, (d) $Cu_{25}Ni_{75}$@NC, and (e) Ni_{100}@NC at various potentials.

Table S3 Summary of the NORR performance of the electrocatalysts in 1M KOH at +0.1 V vs RHE.

Sample	NH_3 yield rate ($\mu mol\ cm^{-2}\ h^{-1}$)	FE_{NH3} (%)
Cu_{100}@NC	0.74	41.83
$Cu_{75}Ni_{25}$@NC	3.6	79.33
$Cu_{50}Ni_{50}$@NC	3.55	65.29
$Cu_{25}Ni_{75}$@NC	3.58	62.98
Ni_{100}@NC	3.02	52.3

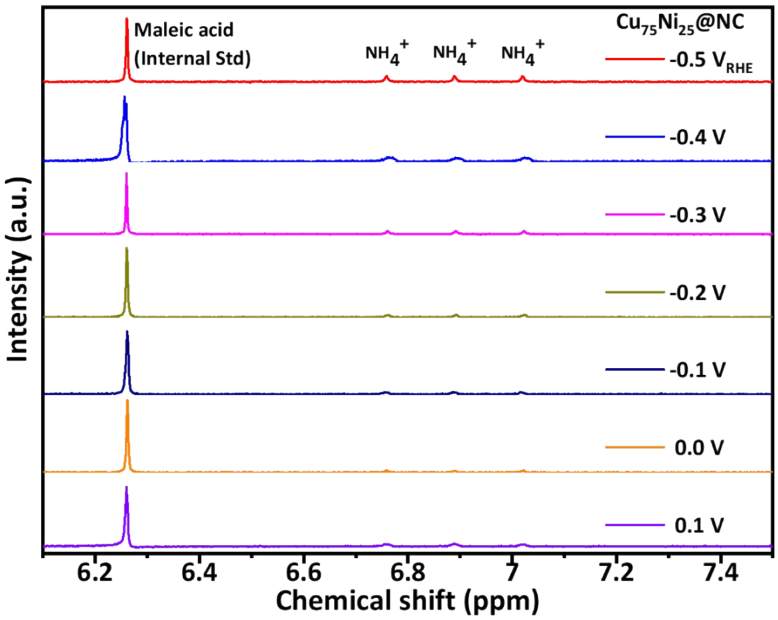

Fig. S19 ^1H NMR spectra of the aliquots collected after 1 h electrolysis of $Cu_{75}Ni_{25}$@NC at various potentials.

Table S4 Comparison of NH_3 yield rates and FE_{NH3} of $Cu_{75}Ni_{25}$@NC catalyst with the reported transition metal catalysts for NORR.

Catalysts	**Electrolyte**	**FE_{NH3} (%)**	**NH_3 yield rate**	**Potential (V vs. RHE)**	**Ref.**
Cu foam	0.25 M Li_2SO_4	93.5	517.1 μmol cm^{-2} h^{-1}	–0.9 V	*Angew. Chem. Int. Ed.* 2020, **59**, 9711-9718
hcp-Co	0.1 M Na_2SO_4	72.58	439.50 μmol cm^{-2} h^{-1}	-0.6 V	*J. Am. Chem. Soc*. 2023, **145**, 6899-6904
$Ru_{0.05}Cu_{0.95}$	0.1 M Na_2SO_4	64.9	17.68 μmol cm^{-2} h^{-1}	-0.5 V	*Sci. China. Chem.* 2021, **64**, 1493-1497
Cu-Ti	0.05 M Na_2SO_4	90	400 μmol cm^{-2} h^{-1}	-0.6 V	*ChemElectroChem.* 2022, **9**, e202101273
Ru-LCN	0.5 M Na_2SO_4	65.96	45.02 μmol cm^{-2} h^{-1}	-0.2 V	*ACS Energy Lett.* 2022, **7**, 1187−1194
Cu@Co	0.1 M Na_2SO_4	76.54	36.89 μmol cm^{-2} h^{-1}	-0.5 V	*Adv. Mater.* 2023, 2309470
CuFe DS/NC	0.1 M Na_2SO_4	90	112.52 μmol cm^{-2} h^{-1}	-0.6 V	*Adv. Mater.* 2023, **35**, 2304646
NiNC@CF	0.5 M PBS	87	94 μmol cm^{-2} h^{-1}	-0.5 V	*J. Mater. Chem. A* 2022, **10**, 6470
Fe/C	0.5 M PBS	77	908 μmol cm^{-2} h^{-1}	-0.6 V	*ACS Energy Lett.* 2022, **7**, 958.
Ni@NC	0.1 M HCl	72.3	34.6 μmol cm^{-2} h^{-1}	0.16 V	*Adv. Sci.* 2022, **9**, 2201410
$CoNi_{(5:5)}O_x$@Cu	1 M KOH	100	20 mg h^{-1} cm^{-2}	-0.68	*Adv. Energy Mater*. 2023, **13**, 2204231.
$Cu_{75}Ni_{25}$@NC	**1 M KOH**	**79**	**3.6 μmol h^{-1} cm^{-2}**	**0.1 V**	**This work**

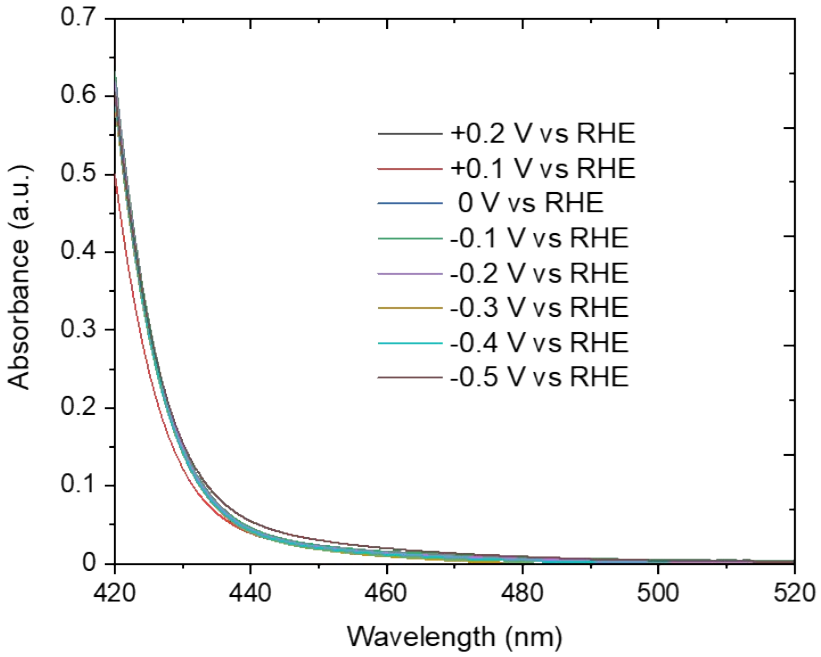

Fig. S20 UV-visible spectra of aliquots collected after 1 h electrolysis of $Cu_{75}Ni_{25}$@NC at various potentials for N_2H_4 detection.

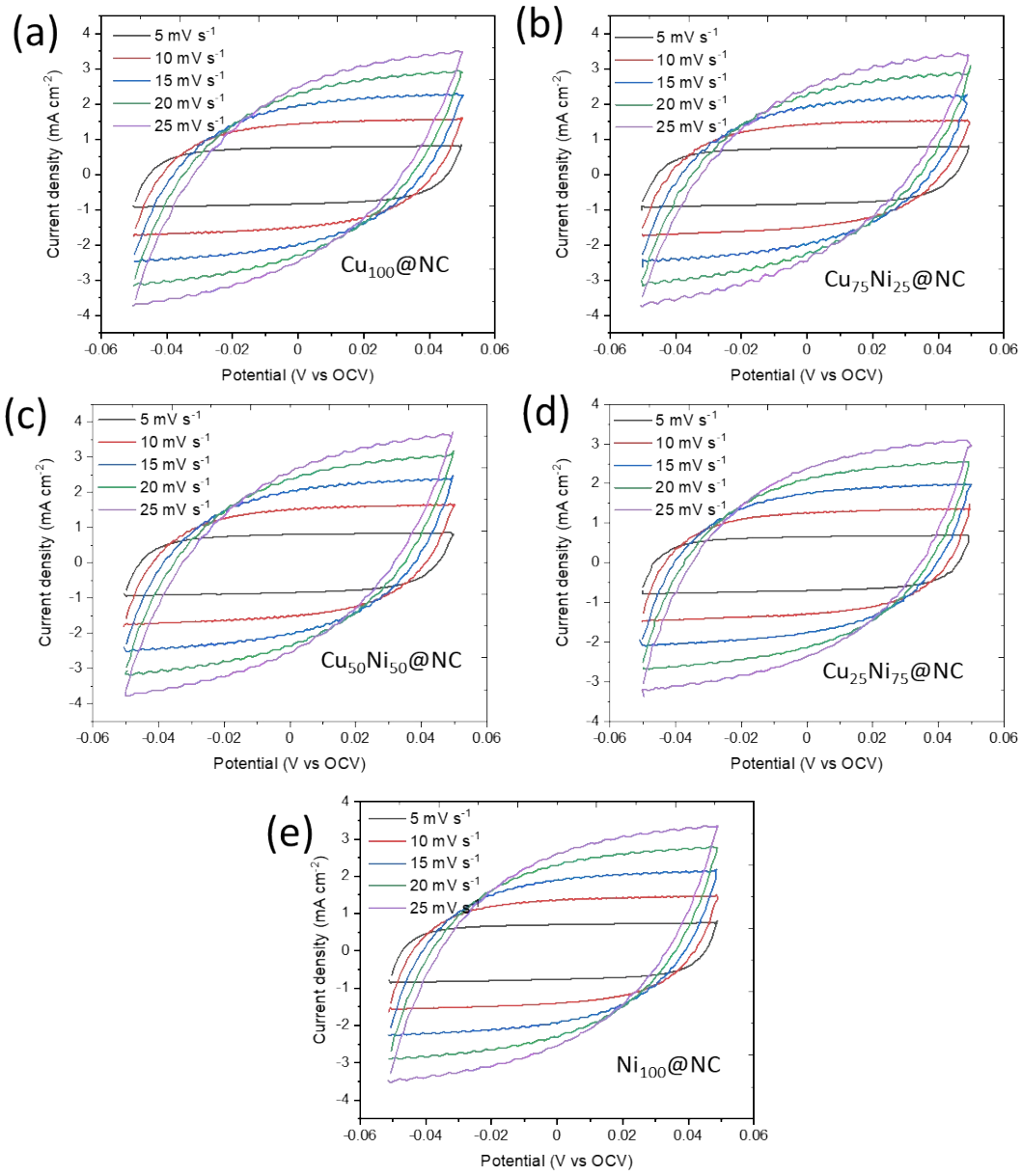

Fig. S21 The cyclic voltammograms of (a) Cu_{100}@NC, (b)$Cu_{75}Ni_{25}$@NC, (c) $Cu_{50}Ni_{50}$@NC, (d) $Cu_{25}Ni_{75}$@NC, and (e) Ni_{100}@NC at different scan rates.

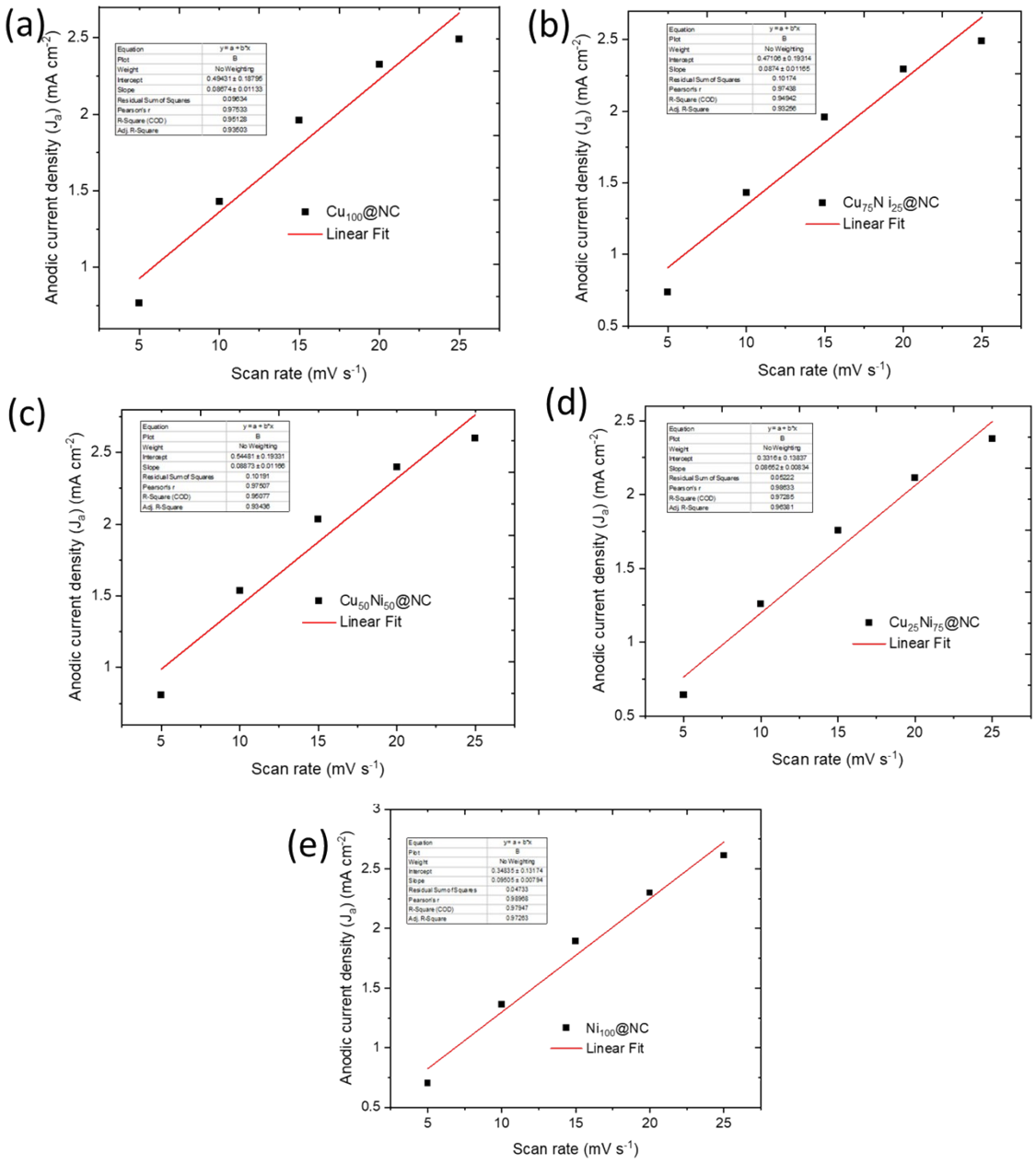

Fig. S22 The anodic current density vs scan rate plots for the estimation of double layer capacitance (C_{dl}) of (a) Cu_{100}@NC, (b)$Cu_{75}Ni_{25}$@NC, (c) $Cu_{50}Ni_{50}$@NC, (d) $Cu_{25}Ni_{75}$@NC, and (e) Ni_{100}@NC.

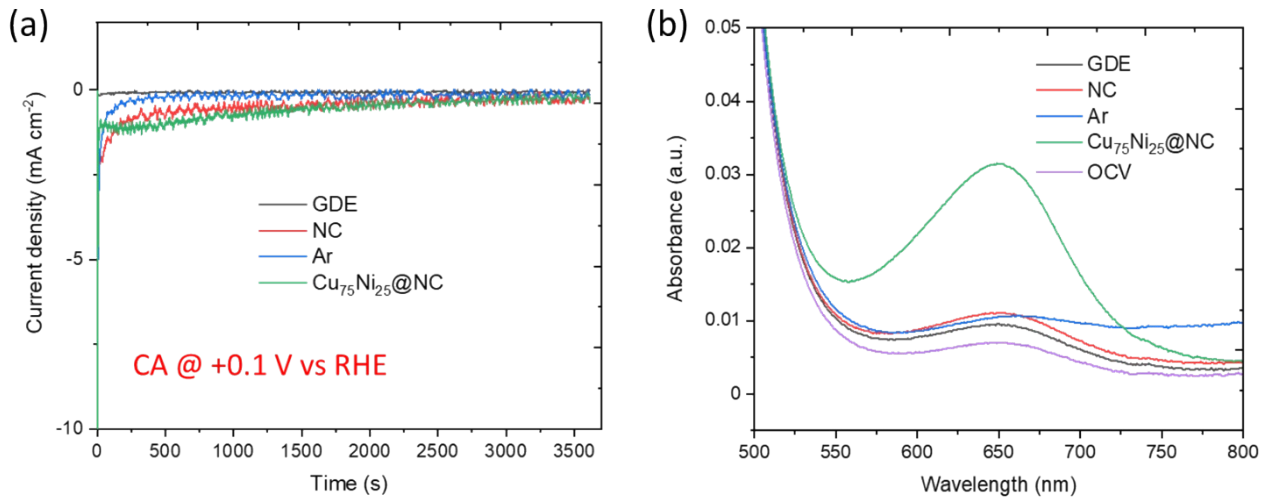

Fig. S23 (a) CA curves of various controlled experiments performed at +0.1 V vs. RHE, and (b) The corresponding UV-visible spectra for NH_3 detection.

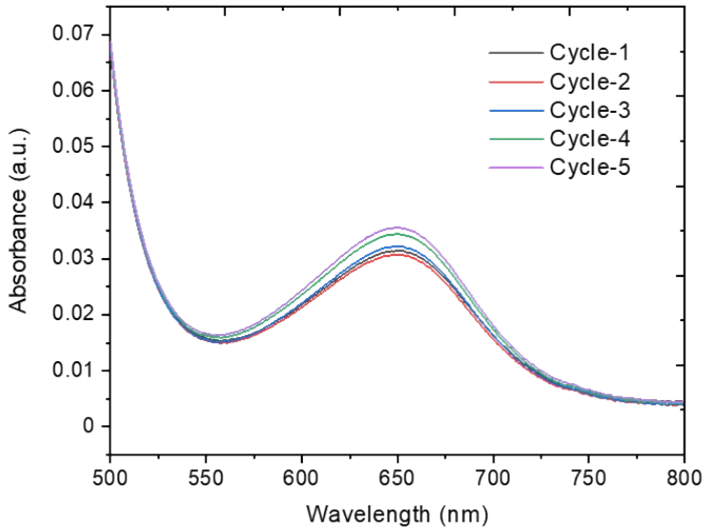

Fig. S24 The UV-visible spectra of the aliquots collected during the cyclic stability test of $Cu_{75}Ni_{25}$@NC.

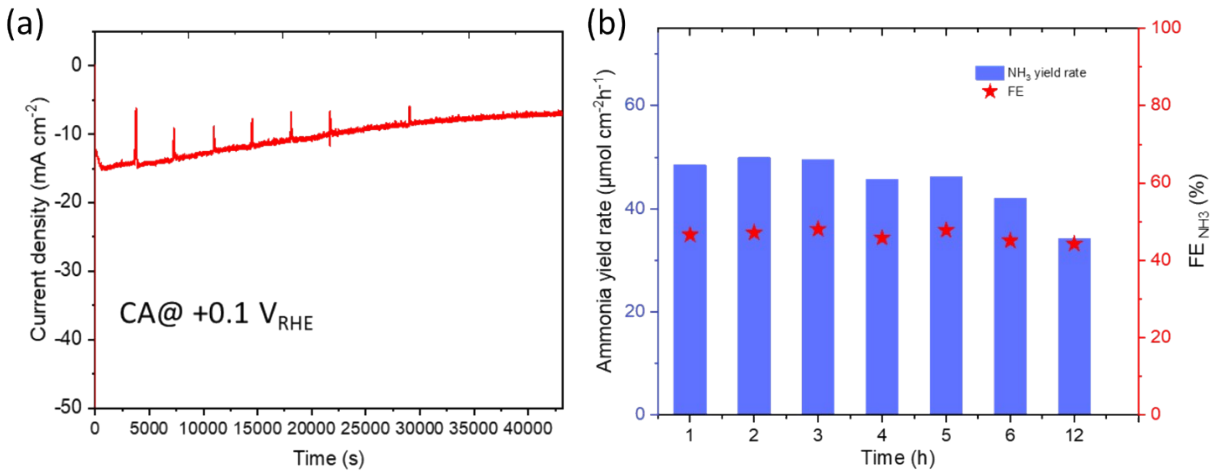

Fig. S25 (a) Long term stability (with continuous NO flow) test of $Cu_{75}Ni_{25}$@NC, and (b) The corresponding NH_3 yield rate and FE_{NH3} at different time intervals.

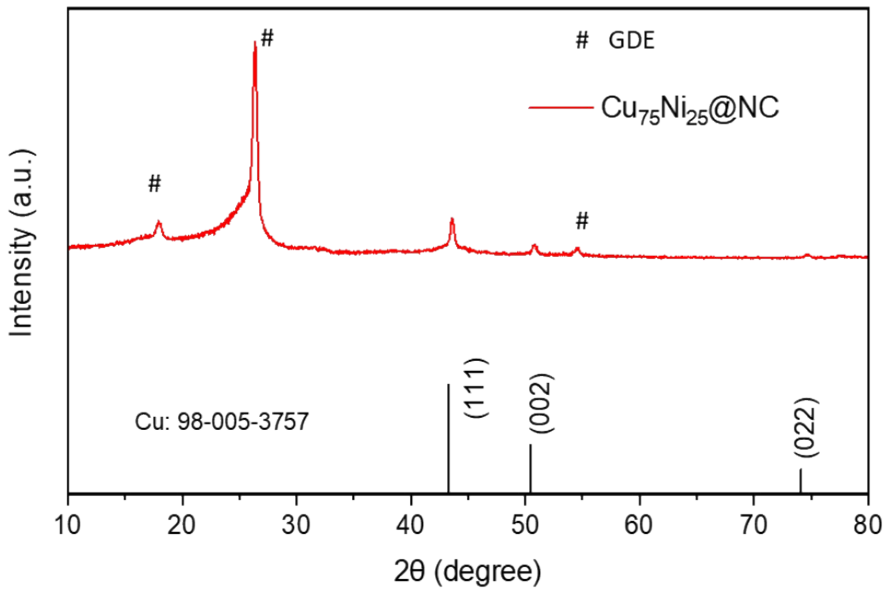

Fig. S26 PXRD pattern of the GDE supported $Cu_{75}Ni_{25}$@NC after the stability test.

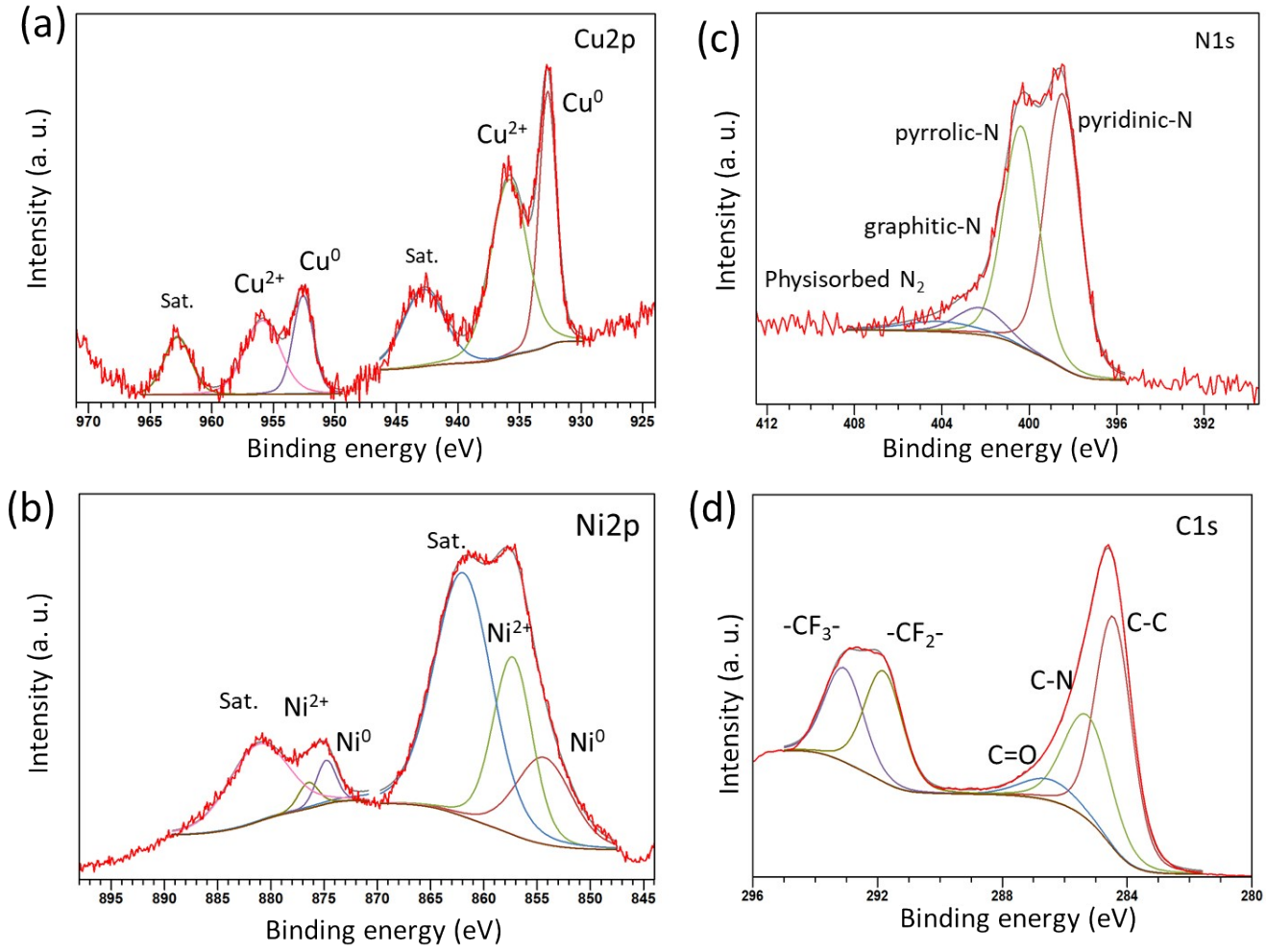

Fig. S27 Deconvoluted XPS spectra of (a) Cu2p, (b) Ni2p, (c) N1s, and (d) C1s of $Cu_{25}Ni_{75}$@NC after the stability test.

Table S5 ICP-OES analysis of $Cu_{75}Ni_{25}$@NC before and after the electrolysis.

Sample	Cu (ppm)	Ni (ppm)	Cu (mM)	Ni (mM)	Cu: Ni ratio
$Cu_{75}Ni_{25}$@NC (Fresh)	0.139	0.027	0.0021	0.00046	4.5: 1
$Cu_{75}Ni_{25}$@NC (Post)	0.133	0.03	0.0020	0.0005	4: 1

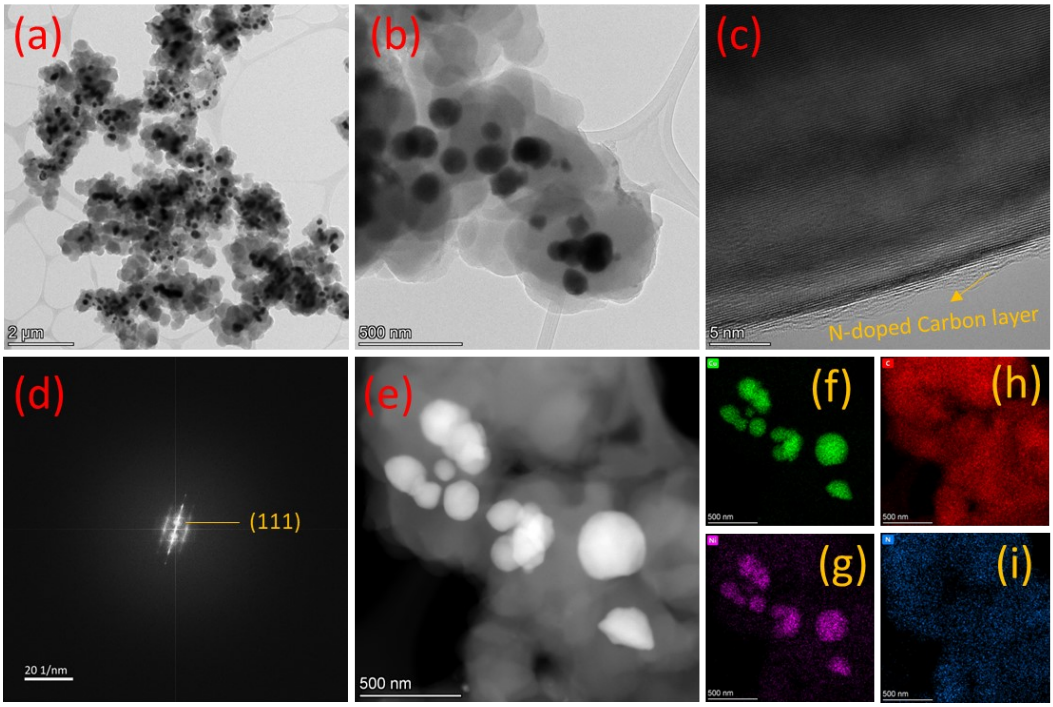

Fig. S28 TEM analysis of $Cu_{75}Ni_{25}$@NC after stability test. (a-b) TEM images. (c) HRTEM image and (d) the corresponding FFT pattern. (e) HAADF image and (f-i) elemental mapping.

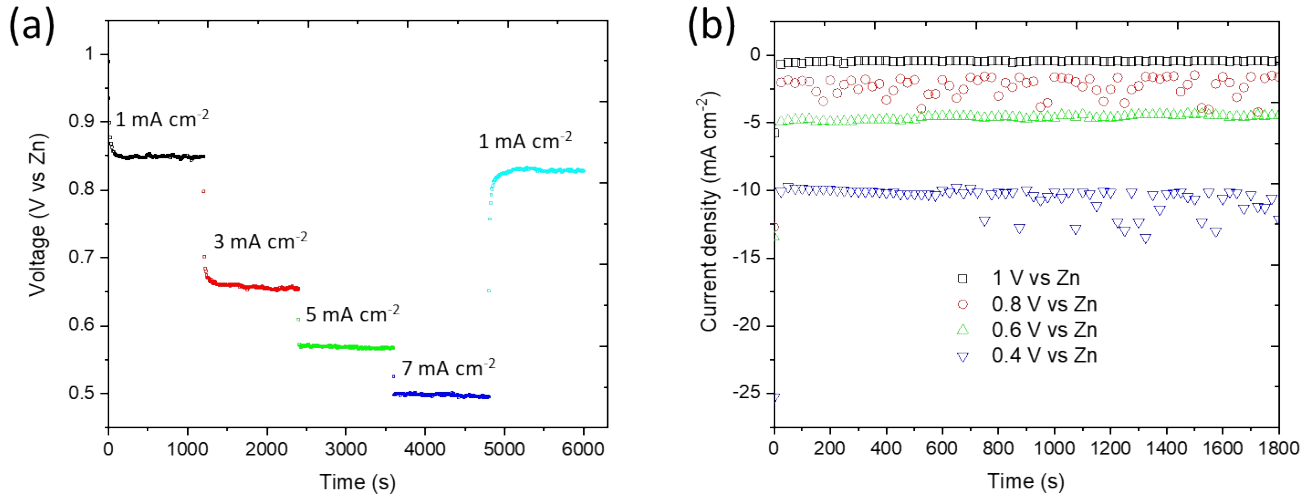

Fig. S29 (a) Discharge curves of Cu_{100}@NC based Zn-NO battery at different current densities. (b) Discharge current densities of Cu_{100}@NC based Zn-NO battery at different voltages.

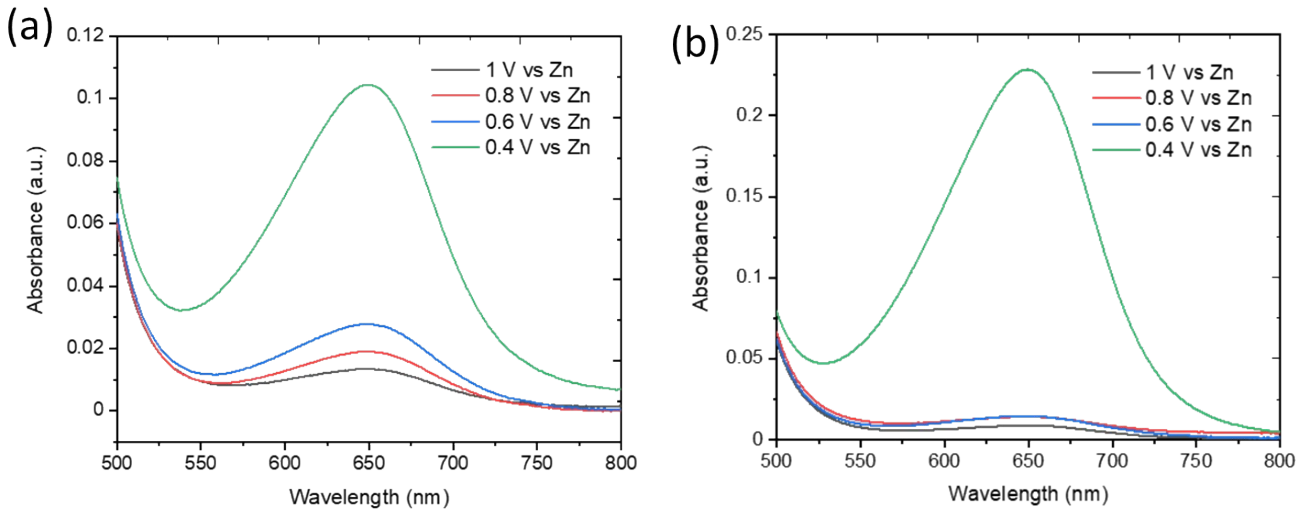

Fig. S30 UV-visible spectra of aliquots collected after 30 min discharge of (a) $Cu_{75}Ni_{25}$@NC and (b) Cu_{100}@NC based Zn-NO batteries at various potentials.

Table S6 Comparison of NH_3 yield rate and peak power density of our Zn-NO battery with the reported Zn-N_2, and Zn-NO batteries.

Cathode	**Battery systems**	**Power density (mW cm^{-2})**	**Ref.**
Cu NPs	Zn-N_2	0.0101	*Chem. Commun.* 2019, **55**, 12801
CoPi/NPCS	Zn-N_2	0.49	*ACS Appl. Mater. Interfaces* 2021, **13**, 12106
NbS_2	Zn-N_2	0.31	*Appl. Catal. B: Environ.* 2020, **270**, 118892
$Fe_{1.0}$HTNs	Zn-N_2	0.0276	*J. Mater. Chem. A* 2021, **9**, 4026-4035.
a-$B_{2.6}C$@TiO_2/Ti	Zn-NO	1.7	*Angew. Chem. Int. Ed.* 2022, **61**, e202202087
Ni_2P nanoarray	Zn-NO	1.53	*J. Mater. Chem. A* 2021, **9**, 24268
MoS_2/GF	Zn-NO	1.04	*Angew. Chem. Int. Ed.* 2021, **133**, 25467
CuFe DS/NC	Zn-NO	2.30	*Adv. Mater.* 2023, **35**, 2304646
Cu@Co	Zn-NO	3.08	*Adv. Mater.* 2023, 2309470
$Cu_{75}Ni_{25}$@NC	**Zn-NO**	**3.8**	**This work**